Facile investigation of reversible nanostructure changes in flexible crystals

Shotaro Hayashi (hayashi.shotaro@kochi-tech.ac.jp)
Kochi University of Technology https://orcid.org/0000-0001-8703-6740

Article

Keywords: flexible crystals, nanostructure changes, X-ray diffraction analysis

Posted Date: September 14th, 2020

DOI: https://doi.org/10.21203/rs.3.rs-71849/v1

Abstract

Detailed investigation of macroscopic deformation and nanoscopic structural changes in flexible organic crystals pose challenges for investigators. Herein, applied stress and subsequent relaxation of elastic organic crystals resulted in reversible macroscopic crystal deformation. X-ray diffraction with a curved jig revealed reversible nanoscopic structural changes in the crystal structure under the bending stress and relaxation. The crystal lattice changed quantitatively under the applied macroscopic stress-strain (%). This method enables quantitative monitoring of the dynamic nanoscopic structural changes in detail associated with crystal deformation through the use of standard laboratory X-ray diffraction analysis. Importantly, the developed method offers a way of quantitatively measuring reversible structural changes, without synchrotron X-ray analysis. Moreover, the analysis derives Poisson's ratio, i.e., the ratio of the change in the width per unit width of materials. It is important in materials science, normally has a positive value in the range of 0.2–0.5. However, the crystals show not only the "Poisson effect" but also the unusual "negative Poisson effect". This novel approach for investigation generates unprecedented opportunities for understanding dynamic nanostructure changes in flexible organic crystals.

Introduction

Organic crystals are typically poorly elastic and tend to be either brittle or plastically deformable.[1-5] Unlike entropic elasticity, in which an ordered molecular assembly returns to an unordered state according to the second law of thermodynamics, enthalpic elasticity involves a restoring force derived from a change of molecular array spacing induced by an external force and energy.[6,7] Elastically deformable organic crystals (elastic organic crystals)[8-22] have enthalpic elasticity, which alters intermolecular packing through mechanical deformation of the crystals.[8-14] There is a need to investigate changes of the nanoscopic structural molecular arrangement space (or lattice) in a crystal under deformation stress. Spatially resolved X-ray diffraction measured at different regions of a bent elastic crystal from the outer part of an elongated arc to the inner contracted arc is an effective method of structural investigation, as reported by Clegg and McMurtrie.[15] In the case of fluorescent elastic organic crystals, deformation-induced fluorescence changes also enable intermolecular packing information to be predicted from spatially resolved emission spectra.[16] Raman spectroscopy is also effective for tracking changes in intermolecular interactions.[17,18] However, synchrotron X-ray analysis is necessary to characterize nanoscopic structural changes associated with crystal bending deformation in detail,[15] which limits the accessibility of such measurements. In addition, there are currently no simple readily accessible methods to quantitatively determine the degree of a nanoscopic change with respect to the amount of deformation (strain, %).

Here, we examine a fluorescent donor-acceptor elastic organic crystal based on the screening of cyano-β-oligo(phenylenevinylene)s. To develop a simple measurement of the nanoscopic structural changes with respect to curvature (strain, %), the diffraction patterns at the crystal interface were examined. One-dimensional (1D) X-ray diffraction (XRD) analysis, which is readily accessible, was used to determine the

degree of nanoscopic structural change with respect to the macroscopic deformation amount (%) calculated from the stress-strain owing to the crystal bending curvature. Quantitative deformation and nanoscopic changes revealed that the crystal cell unit had a negative Poisson effect.[23] This is the first time a mechanical deformation phenomenon has been reported for an organic crystalline material.

Results And Discussion

Fabrication of elastic organic crystals. Synthesis of β-COPVs was performed by Knoevenagel condensation of aryl dicarboxaldehyde with aryl acetonitrile in the presence of a strong base.[24] As a result of screening, an elastic organic crystal based on the molecule with a methoxyphenylene core and bromophenyl end groups (Fig. 1a) was obtained from 4-bromobenzyl cyanide and 2,5-dimethoxybenzene-1,4-dicarboxaldehyde.[25] Reddish orange-colored needle-like crystals were grown from 1,2-dichloroethane (Fig. 1b). The optical properties, i.e., UV-vis absorption (λ_{abs}) and emission (λ_{em}) wavelengths, full-width half-maximum (FWHM), absolute fluorescence quantum yield (Φ_F), fluorescence lifetime (τ), and radiative (k_r) and nonradiative (k_{nr}) decay rate constants, were measured from solution and crystals. The β-COPV with methoxy groups on the phenylene core exhibited charge transfer (CT) interactions. UV-vis absorption spectrum showed two peaks corresponding to π-π* and CT transitions (Fig. 1c). The emission spectrum of the crystal was red-shifted compared with that in CH_2Cl_2 (ca. +100 nm) owing to formation of an intermolecular donor-acceptor system and a more planar π-system (Fig. 1c). The compound had a higher quantum yield (Φ_F) in its crystal form ($\Phi_F = 0.95$) than in CH_2Cl_2 solution ($\Phi_F = 0.41$) owing to suppression of nonradiative processes from the excited state. Moreover, the emission spectrum of the crystal was very narrow, with a FWHM of 65 nm, which was much smaller than that in solution (74 nm). When compared with the solution results (*e.g.*, CH_2Cl_2: $k_r = 1.86 \times 10^8\ s^{-1}$, $k_{nr} = 2.68 \times 10^8\ s^{-1}$), the crystal had a comparable k_r of $2.38 \times 10^8\ s^{-1}$ but a much smaller k_{nr} of $0.12 \times 10^8\ s^{-1}$. The suppression of k_{nr} likely contributed to the enhanced Φ_F of the crystal. These results suggest that the desired intermolecular interactions in crystal produced efficient and low-energy emission.

The crystal structure of the molecule is shown in Fig. 2 (triclinic, space group = *P*-1). The torsion angle (θ) between the core Ar_1 and terminal Ar_2 units is 19.37° (Figs. 2a and 2b). The packing of the molecules has a slip-stacked assembly along the *a*-axis that results in close π-π-stacking interactions (l_p = 0.3651 nm) (Fig. 2c). The center-to-center distance of the molecular planes (l_s) is 0.2798 nm. The fibril lamella morphology originates from the slip-stacked molecular packing wires through the self-assembly of planar molecules (Fig. 2c).

Elastic bending for macroscopic deformation. Individual crystals were mechanically tested to assess their elastic properties (Fig. 3a and Supplementary Video S1). A single crystal (thickness: 168 μm, width: 320 μm, length: 12 mm) was fixed to a metal pin with adhesive. Figure 3b and Video 1 show the mechanical bending–relaxation performance of the crystal. Bending stress was applied by pushing the crystal with a glass plate. The straight crystal bent under an applied stress in the c direction and then recovered its original shape upon releasing the stress. Notably, the reversible bending–relaxation of the

crystal could be repeated many times (Figs. 3b-l). This mechanical behavior clearly indicates that the crystal is an elastic (bendable) organic single crystal. The crystal bending angle exceeded 70° (Fig. 3k). The elastic organic crystals did not exhibit slipping between the planes and on visual inspection there was no detectable change in the angle between the ends of the crystals. Thus, the crystal underwent elongation at the outside and contraction at the inside of the bend (Supplementary Fig. S1). The elastic strain (ε_n) of the crystal in the *c*-direction was estimated from the curvature of the bent crystal and the equation $\varepsilon_n = d/2r$, where d corresponds to the width of the (001) plane (d = 168 μm) and r is the radius. The values of ε_n were 1.02%, 1.19%, 1.40%, 1.70%, and 2.80% (Figs. 3c, 3 g, 3i, and 3 k). In contrast, the crystal did not bend under an applied stress in the *b*-direction, *i.e.*, the elasticity was limited to one direction (directional-specific elasticity). Figure 3m schematically illustrates the elastic bending test using a pair of tweezers and a needle. The crystal bent without breaking when the (001) plane was face-up and the bent crystal quickly recovered its original straight shape without any breaking or crack formation upon withdrawal of the force (Figs. 3n and 3o). In contrast, under elastic bending, when the (010) plane was face-up the crystal was brittle (Figs. 3p and 3q). In this case, the inflexible crystal fractured. This direction-depended elasticity is related to anisotropy of the molecular arrangement in the crystal (Fig. 2c).

X-ray analysis of nanoscopic structural changes. To link the directivity of the crystal to its crystal structure, one-dimensional (1D) X-ray diffraction (XRD) analysis of the crystal was performed with an original set-up (Supplementary Fig. S2). Patterns derived from the lamellar structure for the *c*-axis were detected when the crystal was positioned parallel to the substrate (Fig. 4a). The Bragg equation was used to calculate the length of the original crystal (010) face up to be 12.367 Å (7.12°), which corresponds to one lamellar layer in the *c*-direction (Fig. 4b). Thus, the face parallel to the substrate is the (001) face. To determine the changes in the structure induced by bending and relaxation, 1D XRD analysis of the front and back of the straight (original and relaxed) and bent crystal was conducted by performing measurements with the crystal set at different curvatures (Fig. 4a). The elastic strain (ε_n) of the crystal in the *c*-direction was also estimated from the width of the (001) plane (d = 168 μm) and the radius (r = 3, 5, and 7 mm) of the curved jigs. Upon bending (ε_n = 1.2%), the patterns at the front of the crystal shifted to a lower angle (7.04°), which corresponded to a distance of 12.556 Å (Fig. 4b). The patterns returned to their original positions upon releasing the stress. Upon re-bending (ε_n = 1.68%), the patterns shifted to an even lower angle (6.98°, 12.657 Å). Recovery of the pattern upon relaxation was also observed. In the case of a greater bending (ε_n = 2.8%), a further shift to a low angle was observed at the front of the crystal (6.94°, 12.723 Å). Furthermore, the patterns from the back of the bent crystal (ε_n = 0.84%), shifted to a higher angle (7.18°, 12.303 Å). These analyses point to a change of the lamellar distance in the *c*-direction, $d_0 \rightarrow d_x$ upon bending (Fig. 4c).

Plots of strain (%) from curvature [$\Delta\varepsilon_{(100)}$] against the degree of change, $\Delta\varepsilon_{(001)}$, from XRD results, and ε_n showed a correlation between strain and the change of lamellar distance (Fig. 4d). Hence, the elongation or contraction in the *a*-direction induced elongation or contraction in the *c*-direction, respectively (Fig. 4e). The calculated Poisson's ratio, v, is defined as the ratio of the change in the width per unit width of materials (plastics, metals), to the change in its length per unit length, as a result of strain. Typically, v

values are in the range of 0.2–0.5 associated with a contraction of the width of a material when it is stretched (Fig. 4f). Here, the *v* value of the cell unit (001) can be estimated from the *a*-axis elongation, as calculated from the bending strain and the variation ratio of *c*-axis: $v_{(001)} = -\Delta\varepsilon_{(001)} / \Delta\varepsilon_{(100)}$.[16] Notably, the $v_{(001)}$ value of this crystal was approximately − 1.0 (Fig. 4d). A negative value of Poisson's ratio (*negative* Poisson effect) represents an unusual deformation mode in material science,[18] but characteristic examples are based on molecularly dense and well-organized organic crystals.

To investigate the applicability of this method to other crystals, similar measurements were performed for an elastic 9,10-dibromoanthracence crystal. A reversible peak shift occurred as the shape changed from straight to bent (Supplementary Fig. S3a). Importantly, the degree of change in the peak shifts of $[\Delta\varepsilon_{(001)}]$ and $[\Delta\varepsilon_{(100)}]$ changed with the curvature. In this crystal, contraction of the *c*-axis occurred rather than elongation of the *a*-axis. However, because elongation of the *c*-axis occurred with respect to contraction for *a*-axis, the behavior was different from that of the elastic β-COPV crystal (Supplementary Figs. S3b and S3c). Hence, this crystal showed a typical Poisson effect with a $v_{(001)}$ value of 0.23–0.25.

Conclusion

A simple method is developed for quantitative investigation of reversible nanoscopic structural changes in flexible crystals. Mechanically reversible bending deformation causes a nanoscopic structural change in an elastic organic crystal based on the novel π-conjugated molecule, β-COPV. The nanoscopic lattice structure in a crystal changed under the applied macroscopic stress-strain (%). This method enables the nanoscopic structural changes associated with crystal bending deformation to be quantitative analyzed with readily available X-ray equipment. Notably, the calculated Poisson's ratio of the crystal for the (001) face was approximately − 1.0, which is unusual among common materials (approximately 0.2–0.5). Hence, this material showed a negative Poisson effect, suggesting the mechanical characteristics of a dense and well-organized organic crystal structure. Similarly, deformation and structural changes were observed for 9,10-dibromoanthracence crystals, which should a showed normal Poisson effect (approximately 0.24). This work opens new avenues for structural investigations of flexible crystals. This is simple method that will be of great utility to researchers who cannot readily access synchrotron X-ray diffraction facilities.

Declarations

Acknowledgements

S. H. acknowledges the Japan Society for the Promotion of Science (JSPS), KAKENHI for a Grant-in-Aid for Scientific Research B (no. 18H02052) and Grant-in-Aid for Scientific Research on Innovative Areas ('π-figuration': no. 17H05171, 'Coordination asymmetry': no. 19H04604 and 'Soft Crystals': no. 20H04684). This work was performed under the Cooperative Research Program of the "Network Joint Research Center

for Materials and Devices". We thank Andrew Jackson, PhD, from Edanz Group (https://en-author-services.edanzgroup.com/ac) for editing a draft of this manuscript.

References

1. Saha, S., Mishra, M. K., Reddy, C. M. & Desiraju, G. R. From molecules to interactions to crystal engineering: mechanical properties of organic solids. *Acc. Chem. Res.* 51, 2957–2967 (2018).
2. Reddy, C. M., Kirchner, M. T., Gundakaram, R. C., Padmanabhan, K. A. & Desiraju, G. R.; Isostructurality, polymorphism and mechanical properties of some hexahalogenated benzenes: the nature of halogen···halogen interactions. *Chem. Eur. J.* 12, 2222–2234 (2006).
3. Panda, M. K., Ghosh, S., Yasuda, N., Moriwaki, T., Mukherjee, G. D., Reddy, C. M. & Naumov, P. Spatially resolved analysis of short-range structure perturbations in a plastically bent molecular crystal. *Nat. Chem.* 7, 65–72 (2015).
4. Catalano, L., Karothu, D. P., Schramm, S., Ahmed, E., Rezgui, R., Barber, T. J., Famulari, A. & Naumov, P. Dual-mode light transduction through a plastically bendable organic crystal as an optical waveguide. *Angew. Chem. Int. Ed.* 57, 17254 – 17258 (2018).
5. Bhattacharya, B., Roy, D., Dey, S., Puthuvakkal, A., Bhunia, S., Mondal, S., Chowdhury, R., Bhattacharya, M., Mandal, M., Manoj, K., Mandal, P. K. & Reddy, C. M. Mechanical bending induced fluorescence enhancement in plastically flexible crystals of a GFP chromophore analogue. *Angew. Chem. Int. Ed.* DOI: 10.1002/ange.202007760.
6. DeRosa, C. & Auriemma, F. From entropic to enthalpic elasticity: novel thermoplastic elastomers from syndiotactic propylene–ethylene copolymers. *Adv. Mater.* 17, 1503–1507 (2005).
7. DeRosa, C. & Auriemma, F. Structure and physical properties of syndiotactic polypropylene: a highly crystalline thermoplastic elastomer. *Prog. Polym. Sci.* 31, 1145–237 (2006).
8. Commins, P., Karothu, D. P. & Naumov, P. Is a bent crystal still a single crystal? *Angew. Chem. Int. Ed.* 58, 10052–10060 (2019).
9. Hayashi, S. Elastic organic crystals of π-conjugated molecules: anisotropic densely packed supramolecular 3D polymers exhibit mechanical flexibility and shape tunability. *Polym. J.* 51, 813–823 (2019).
10. Hayashi, S. & Koizumi, T. Elastic organic crystal of a fluorescent π-conjugated molecule. *Angew. Chem. Int. Ed.* 55, 2701–2704 (2016).
11. Hayashi, S., Asano, A., Kamiya, N., Yokomori, Y., Maeda, T. & Koizumi, T. Fluorescent organic single crystals with elastic bending flexibility: 1,4-bis(thien-2-yl)-2,3,5,6-tetrafluorobenzene derivatives. *Sci. Rep.* 7, 9453 (2017).
12. Hayashi, S., Koizumi, T. & Kamiya, N. Elastic bending flexibility of fluorescent organic single crystal: new aspects of commonly used building block "4,7-dibromo-2,1,3-benzothiadiazole". *Cryst. Growth Des.* 17, 6158–6162 (2017).

13. Hayashi, S., Yamamoto, S., Takeuchi, D., Ie, Y. & Takagi, K. Creating elastic organic crystals of π-conjugated molecules with flexible optical waveguide and bending mechanofluorochromism. *Angew. Chem. Int. Ed.* 57, 17002–17008 (2018).
14. Kenny, E. P., Jacko, A. C. & Powell, B. J. Mechanomagnetics in elastic crystals: insights from [Cu(acac)$_2$]. *Angew. Chem. Int. Ed.* 58, 15082–15088 (2019).
15. Worthy, A., Grosjean, A., Pfrunder, M. C., Xu, Y., Yan, C., Edwards, G., Clegg, J. K. & McMurtrie, J. C. Atomic resolution of structural changes in elastic crystals of copper(II) acetylacetonate *Nat. Chem.* 10, 65–69 (2018).
16. Hayashi, S., Ishiwari, F., Fukushima, T., Mikage, S., Imamura, Y., Tashiro, M. & Katouda, M. Anisotropic poisson's effect and deformation-induced fluorescence change of elastic 9,10-dibromoanthracence single crystals. *Angew. Chem. Int. Ed.* DOI: 10.1002/anie.202006474.
17. Mishra, M. K., Mishra, K., Asif, S. A. S. & Manimunda, P. Structural analysis of elastically bent organic crystals using *in situ* indentation and micro-raman spectroscopy. *Chem. Comm.* 53, 13035–13038 (2017).
18. Wang, K., Mishra, M. K. & Sun, C. C. Exceptionally elastic single-component pharmaceutical crystals. *Chem. Mater.* 31, 1794–1799 (2019).
19. Liu, B., Di, Q., Liu, W., Wang, C., Wang, Y. & Zhang, H. Red-emissive organic crystals of a single-benzene molecule: elastically bendable and flexible optical waveguide *J. Phys. Chem. Lett.* 10, 1437–1442 (2019).
20. Horstman, E. M., Keswani, R. K., Frey, B. A., Rzeczycki, P. M., LaLone, V., Bertke, J. A., Kenis, P. J. A. & Rosania, G. R. Elasticity in macrophage-synthesized biocrystals. *Angew. Chem. Int. Ed.* 56, 1815–1819 (2017).
21. Owczarek, M., Hujsak, K. A., Ferris, D. P., Prokofjevs, A., Majerz, I., Szklarz, P., Zhang, H. Sarjeant, A. A. Stern, C. L. Jakubas, R. Hong, S. Dravid, V. P. & Stoddart, J. F. Flexible ferroelectric organic crystals. *Nat. Commun.* 7, 13108 (2016).
22. Ghosh, S. & Reddy, C. M. Elastic and bendable caffeine cocrystals: implications for the design of flexible organic materials *Angew. Chem. Int. Ed.* 51, 10319–10323 (2012).
23. Lakes, R. From structures with a negative poisson's ratio. *Science* 235, 1038–1040 (1987).
24. Hayashi, S., Hirai, R., Yamamoto, S. & Koizumi, T. A simple route to unsymmetric cyano-substituted oligo(*p*-phenylene-vinylene)s. *Chem. Lett.* 47, 1003–1005 (2018).
25. Hayashi, S., Koizumi, T. & Kamiya, N. 2,5-Dimethoxybenzene-1,4-dicarboxaldehyde: an emissive organic crystal and highly efficient fluorescent waveguide. *ChemPlusChem* 84, 247–251 (2019).

Figures

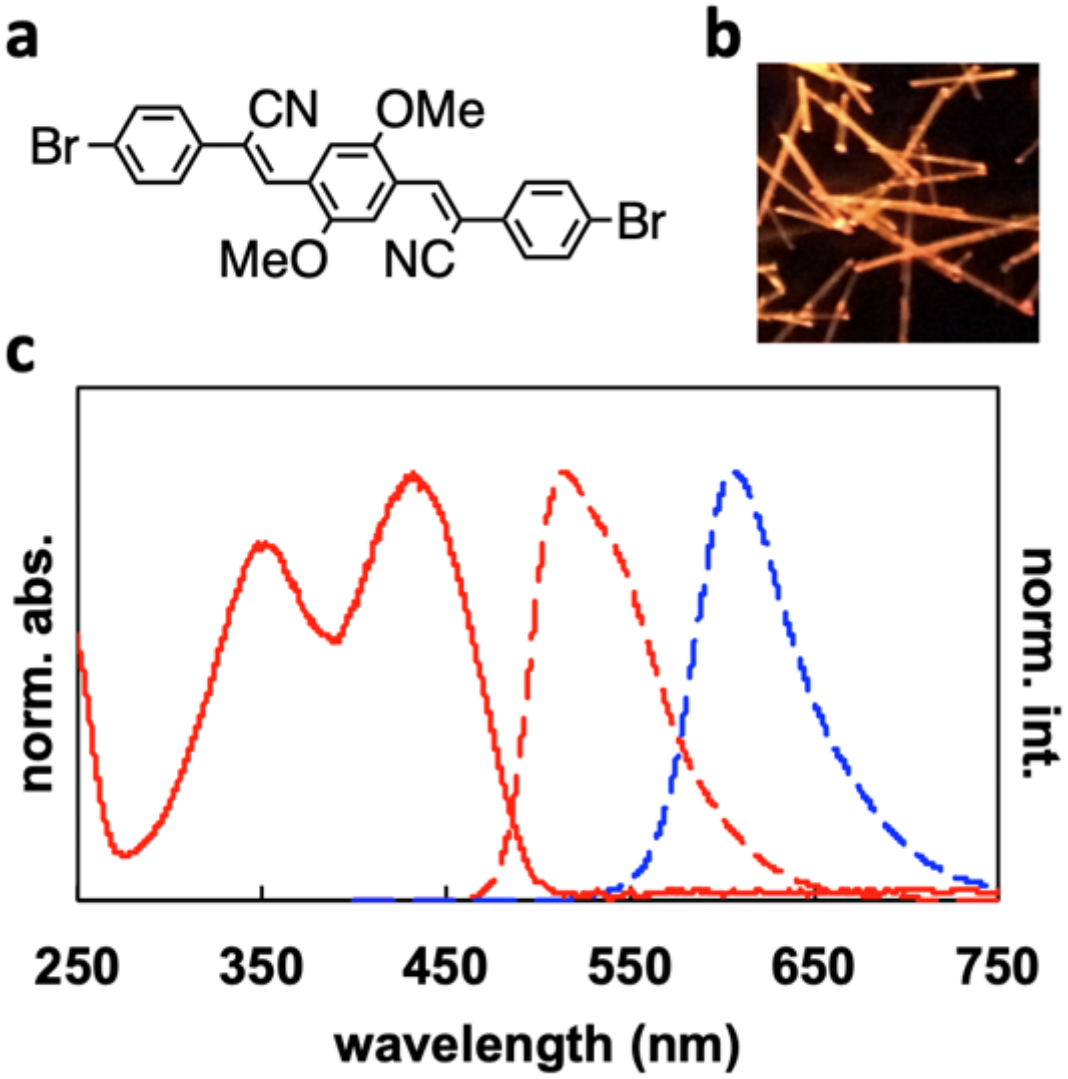

Figure 1

a Chemical structure of β-COPV. b Photograph of crystals under UV irradiation. c UV-vis absorption (solid line) and fluorescence (dotted line) spectra in dichloromethane solution (red line) and from crystal (blue line).

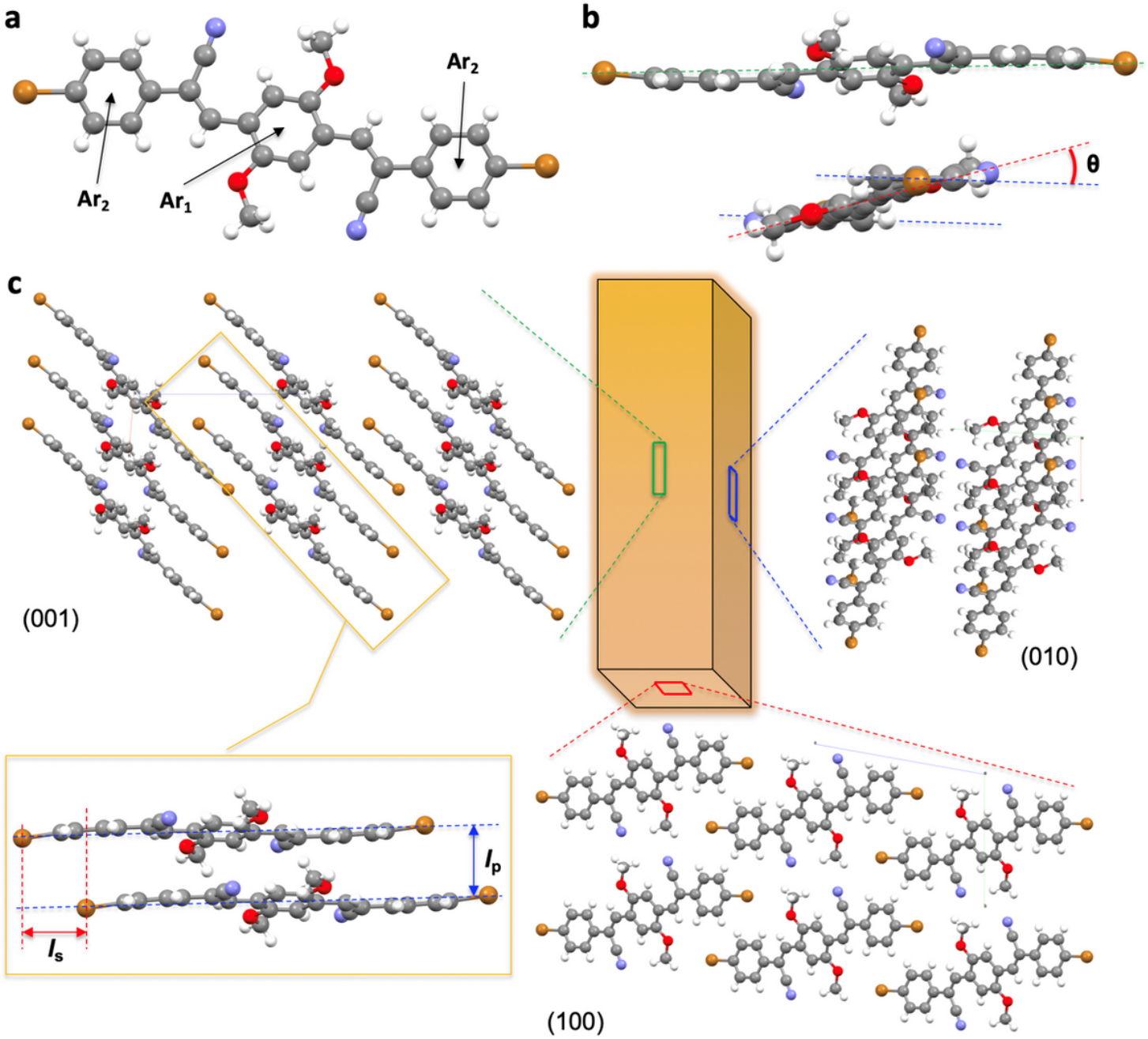

Figure 2

a Crystal structure of β-COPV, top view; b side view; c packing structure.

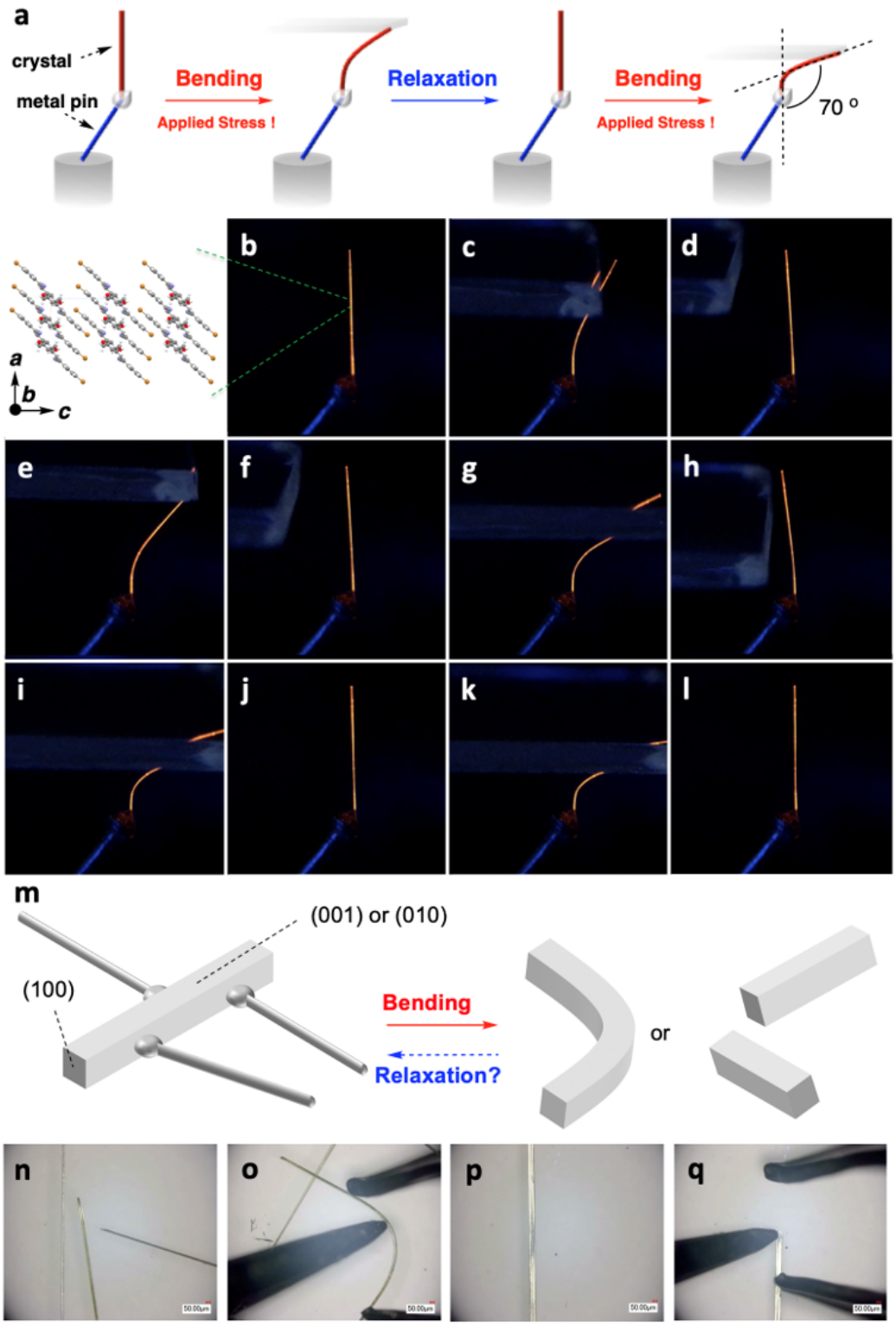

Figure 3

a Schematic illustration of a crystal fixed on a metal pin and subjected to mechanical testing. b-l Photographs of the mechanical bending and relaxation of a β-COPV crystal. Stress was applied by pushing the crystal with a glass plate. Images were captured under UV (365 nm) irradiation. m Schematic illustration of three-point bending test of a crystal. n, o Applied stress of a crystal with (001) face-up. p, q Applied stress of a crystal with (010) face-up.

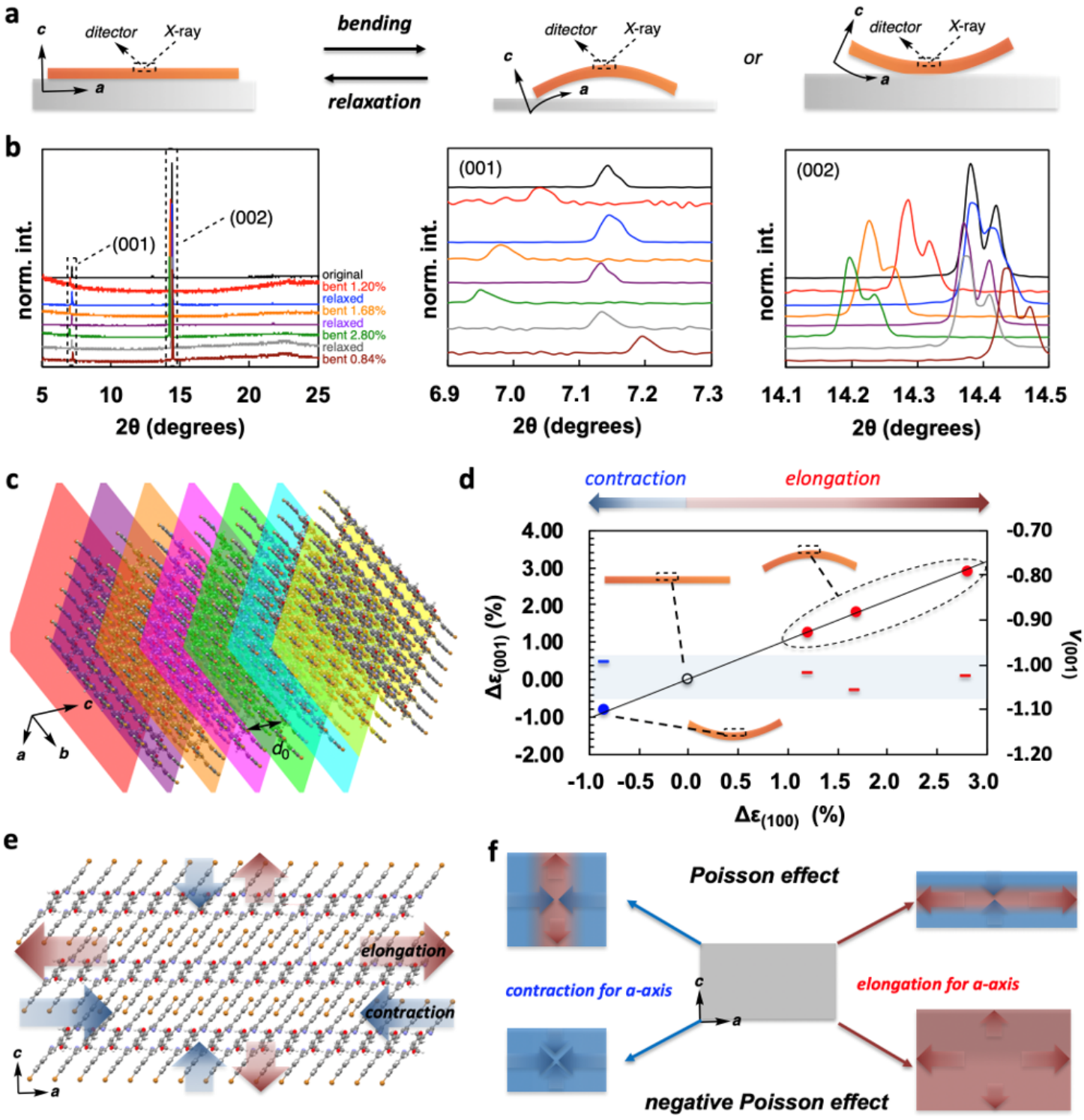

Figure 4

a Schematic illustration of the setup for 1D XRD measurements. b 1D XRD patterns of a β-COPV crystal. c Crystal layer structure of β-COPV. d Plots of elongation/contraction ratio Δε(100), ●, and Poisson's rate ν(001), −, against strain, Δε(010). White: straight and relaxed crystal. Red: front side of bent crystal. Blue: back side of bent crystal. e Schematic illustration of crystal shape and structure change of the crystal plane. f Illustration of the Poisson effect, up, and negative Poisson effect, down.

Supplementary Files

This is a list of supplementary files associated with this preprint. Click to download.

- Video1.mov
- SupportingInformation.docx
- 3bb.cif
- GraphicalContents.png